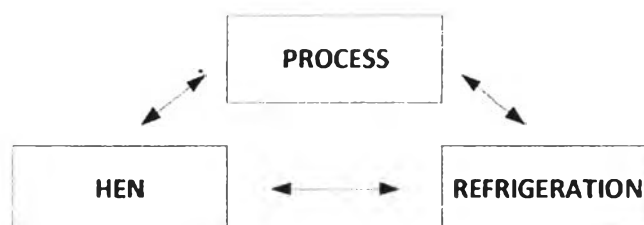


## CHAPTER II

### THEORETICAL BACKGROUND AND LITERATURE REVIEW

In the chemical process industry, there are many processes that operate below ambient temperature. These processes often require heat removal from processes and heat rejection to external agents, such as cooling water or air. Refrigeration systems are employed to supply low temperature cooling. Usually refrigeration are much more expensive than other normal utilities, due to high operating cost and capital intensive compression trains. The operating costs for refrigeration systems are often dominated by the cost of shaft work to drive the compressors. In subambient processes, such as ethylene plants and natural gas liquefaction plants, design of refrigeration systems is the major concern for energy consumption and power consumption.

A subambient process usually comprises of three major parts, namely process, heat exchanger network and refrigeration system, as shown in Figure 2.1



**Figure 2.1** Interaction between three main components.

These systems are all highly interactive and interlinked to each other. Changes in any one of them will cause changes in the other two parts. Any modifications in the process or HEN will have a downstream impact on the shaft work requirement of the refrigeration system. The interactions make the design of refrigeration systems very complex. All design considerations incur trade-offs between energy saving and extra capital investment. Figure 2.2 shows a typical grand composite curve (GCCs) of subambient processes. It gives the whole heat source and sink profile of the process. Further energy saving can be achieved by better heat

integration with processes (Linnhoff, 1991). Therefore, optimal synthesis of refrigeration systems cannot be accomplished without considering the overall context of processes.

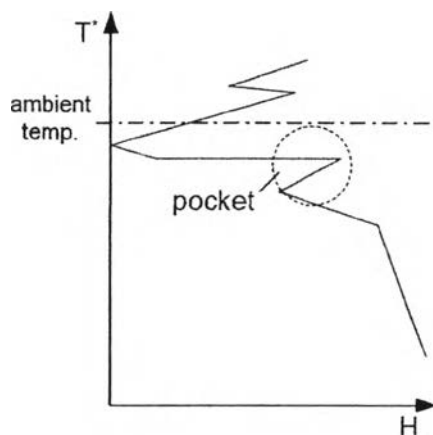


**Figure 2.2** Grand composite curve (GCCs) of subambient processes.

## 2.1 Refrigeration System

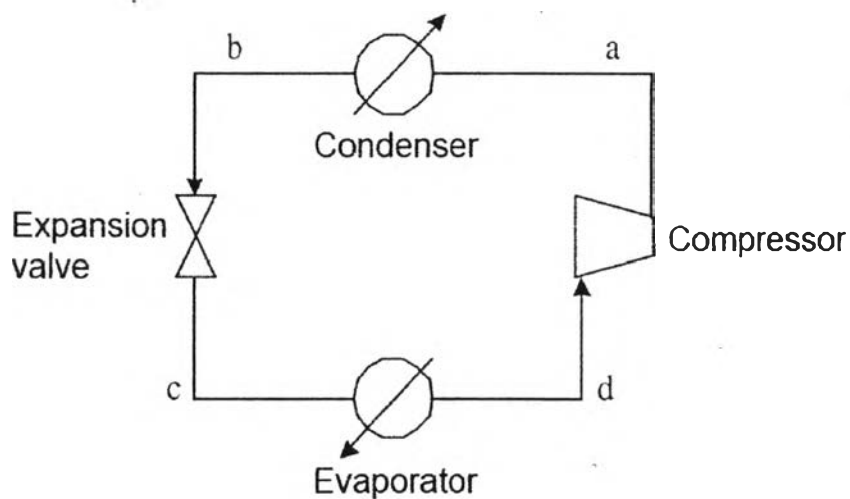


**Figure 2.3** A simple refrigeration cycle flow diagram.

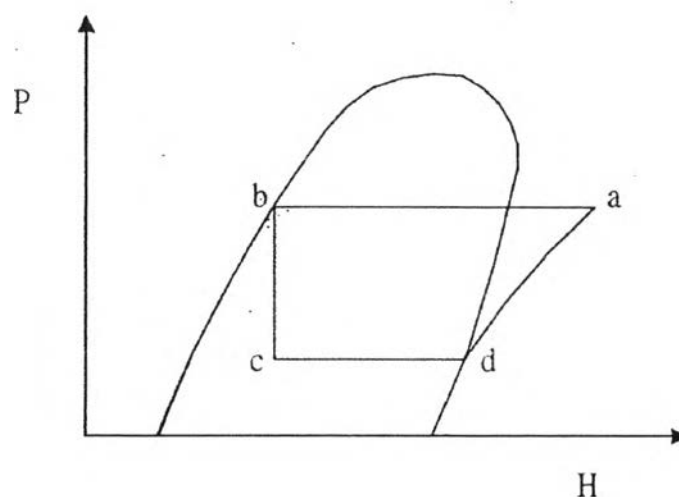


**Figure 2.4** P-H diagram of simple refrigeration cycle.

The refrigeration cycle, as shown in Figure 2.3 and 2.4, consists of four parts: a compressor, a condenser, an evaporator, and an expansion valve.

The saturated refrigerant vapor at point d goes through the compressor after absorbing heat in the evaporator, where the shaft work is consumed and the pressure of the vapor is lifted. The outlet superheated vapor is at point a. The vapor is cooled down in the condenser at constant pressure until it reaches the dew point temperature. Then the saturated vapor is condensed at constant temperature at point b the vapor is converted to saturated liquid. To reach its evaporating temperature at point c, the saturated liquid goes through an expansion valve under an isenthalpic process. From point c to point d, the refrigerant absorbs heat and is evaporated.

When refrigeration is required at very low temperature, a cascade refrigeration system is often used, which consists of two or more cycles and each cycle operates by a different refrigerant. A simple cascade refrigeration system is lower cycle absorbs heat and rejects condensation heat to the upper cycle. The upper cycle absorbs rejected heat from the lower cycle, which is colder than lower. Finally, the heat in the uppermost cycle is rejected to external heat sinks. The reasons for using cascade refrigeration systems are two-folds. First, any single refrigeration cannot cover such a wide refrigeration temperature range. Second, in terms of energy

consumption, using a single refrigerant for the whole refrigeration demand may consume more shaft work than using multiple refrigerants.

Besides suitable operating temperature ranges, there are several considerations for selecting refrigerants. Conventionally, Chlorofluorocarbon (CFC) and Hydrochlorofluorocarbon (HCFC) refrigerants are widely used in domestic refrigerators and automotive air conditioners. But those refrigerants with intermediate to high ozone depletion potential (OPD) will be totally banned in the years to come. Many efforts have already been made to find replacements with similar thermodynamic and transport properties to those banned refrigerants. Factors such as chemical stability, health safety, flammability, and OPD have to be taken into consideration when selecting proper refrigerants to use.

The calculation procedure is performed in three steps:

1. Find the corresponding vapor pressure,  $P_b$  and  $P_c$  by using Antoine equation:

$$\ln P^{vap} = A - \frac{B}{T+C} \quad (2.1)$$

2. Find the outlet temperature,  $T_a$ , of compressor. Most gas compressions follow the adiabatic path, where  $k$  is the isentropic exponent.

$$P \cdot v^k = \text{constant} \quad (2.2)$$

Given the compressor's isentropic efficiency ( $\eta_i$ ), the outlet temperature ( $T_a$ ) can be found by

$$T_a = T_d \left( \frac{\left( \frac{P_a}{P_d} \right)^{\frac{k-1}{k}} - 1}{\eta_i} \right) \quad (2.3)$$

Where,

$$k = \frac{C_p}{(C_p - R)} \quad (2.4)$$

$C_p$  is the average molar heat capacity at  $T_a$  and  $T_d$

3. Calculate the shaft work requirement. An energy balance around the compressor gives the shaft work requirement of compressor:

$$W_{shaft} = m \cdot (h^a - h^d) \quad (2.5)$$

The enthalpy is estimated by using the departure function of Peng-Robinson equation of state:

$$h - h^* = RT(z - 1) + \frac{T \left( \frac{da}{dT} \right) - a}{2\sqrt{2}b} \ln \left[ \frac{Z + (1 + \sqrt{2})B}{Z + (1 - \sqrt{2})B} \right] \quad (2.6)$$

Where,

$$a(T) = 0.45724 \frac{R^2 T_c^2}{P_c} \cdot \alpha \quad (2.7)$$

$$b = 0.07780 \frac{RT_c}{P_c} \quad (2.8)$$

$$\sqrt{\alpha} = 1 + \kappa \cdot \left( 1 - \sqrt{\frac{T}{T_c}} \right) \quad (2.9)$$

$$\kappa = 0.37464 + 1.54226 \cdot \omega - 0.26992 \cdot \omega^2 \quad (2.10)$$

$$\frac{da}{dt} = -0.45724 \frac{R^2 T_c^2}{P_c} \kappa \frac{R^2 T_c^2}{P_c} \quad (2.11)$$

$$B = \frac{bP}{RT} \quad (2.12)$$

Thus, the enthalpy difference can be calculated between two states,  $h^a - h^d$ , by the following relation:

$$h^a - h^d = [h(T_a, P_a) - h^*(T_a, P_0)] + [h^*(T_a, P_0) - h^*(T_d, P_0)] - [h(T_d, P_d) - h^*(T_d, P_0)] \quad (2.13)$$

Where the first and third terms of the right-hand side are computed by the departure function described above, and the second term is the enthalpy difference of ideal gas ( $P_0 = 0$ ) between  $T_a$  and  $T_d$ , which is:

$$h^*(T_a, P_0) - h^*(T_d, P_0) = \int_{T_d}^{T_a} C_p^*(T) dT \quad (2.14)$$

Once the enthalpy difference has been obtained for  $h^a$  and  $h^d$ , the shaft work requirement of the compressor for this simple refrigeration cycle is obtained.

## 2.2 The Subambient Processes

For the case study of subambient process, LNG process is the interested one that is selected to study.

Natural gas is a mixture of components that consists of methane (60-98%) with small amounts of other hydrocarbon fuel components, nitrogen, carbon dioxide, helium, and traces of other gases commonly converted to liquid form for storage at

pressure of 70-500 kPa and around  $-150^{\circ}\text{C}$  or lower. Before natural gas is liquefied, it must be treated by removal of  $\text{CO}_2$  condensate, organic sulfur compounds, and Hg because these contaminants block and damage equipment.

The pretreatment processes consist of four stages. First stage is  $\text{CO}_2$  and  $\text{H}_2\text{S}$  removal stage where  $\text{CO}_2$  would not be exceed 50 ppm in treated natural gas feed otherwise; it was frozen in pipelines of liquefaction process. In the past,  $\text{CO}_2$  removal unit used sulfinol but it was not good because it attracted heavy hydrocarbons and it dragged the heavier to the sulfinol pump allowing the heavy hydrocarbons to vent into the air. The MDEA was used instead of sulfinol because it was cheaper to install and less utility using. Second stage is dehydration, where water was removed from natural gas to avoid water freezing in pipeline. TEG (Triethylene Glycol) was used as primary solvent absorbs water in natural gas in contactor tower. After that gas was passed through molecular sieve to ensure water was removed completely. Third stage is Hg removal unit, where Hg was removed to prevent by using activate bed filter in Hg filtration. Fourth stage is the installation of a duster in pretreatment process outlet to ensure that the natural gas feed was free from small solid particles.

After natural gas pretreatment, it was sent to liquefaction process. There are many processes for natural liquefaction that involved subambient temperature as cryogenic process.

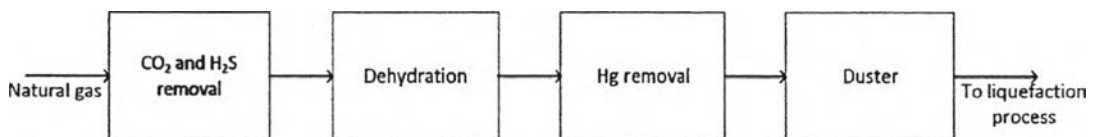
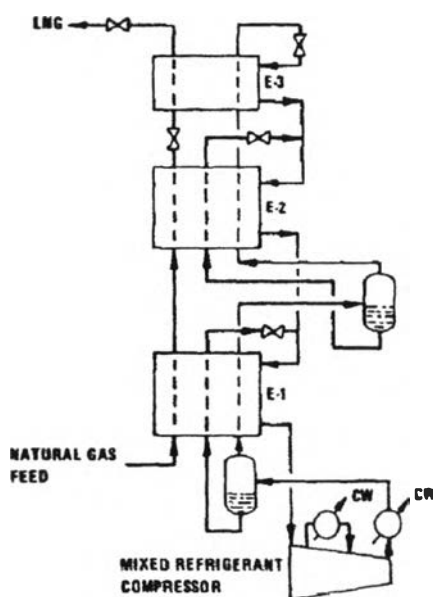


Figure 2.5 Schematic of natural gas pretreatment process.

## 2.2.1 Process of Natural Gas Liquefaction

### 2.2.1.1 Single Mixed Refrigerant Process



**Figure 2.6** Single-pressure mixed refrigerant natural gas liquefaction process (Chiu *et al.*, 1980).

The mixed refrigerant is the mixture of nitrogen and hydrocarbons from methane to pentane. The natural gas feed is cooled in heat exchanger by the high pressure refrigerant. After that, the low pressure refrigerant from exchanger returns to compressor, as shown in Figure 2.6. The refrigerant from discharge of compressor is partially condensed by cooling water and then separated in a phase separator. The liquid phase is subcooled and reduced to suction pressure then joined with refrigerant fraction from E-2. The vapor phase is cooled and separated phase in E-2. (Chiu *et al.*, 1980)

### 2.2.1.2 Propane-Precooled Mixed Refrigerant Process

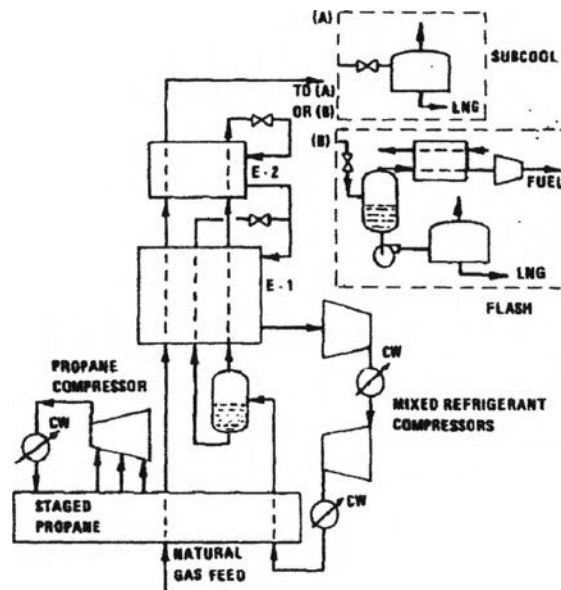


**Figure 2.7** Propane-precooled mixed refrigerant natural gas liquefaction process (Chiu *et al.*, 1980).

The mixed refrigerant and feed stream is pre-cooled by stage propane. The mixed refrigerant has lower boiling range. This combination reduces the boiling range of mixed refrigerant and improves the thermodynamic efficiency. There are two modes for operation. First, subcool mode, the natural gas is liquefied and subcooled to a temperature range around  $-126.67^{\circ}\text{C}$  in cryogenic heat exchanger. Second, flash mode, the natural gas is liquefied at around  $-110^{\circ}\text{C}$  is reduced pressure and flashed. The flash vapor is compressed and sent to fuel system, as shown in Figure 2.7.

Both processes are compared by second law analysis based on exergy (availability). Exergy is the potential for doing work when system is returned to ambient conditions. The alternative systems are compared by exergy loss to determine the most economic process. A comparison between the single pressure mixed refrigerant and propane-precooled mixed refrigerant processes requires the exergy loss where one from the single pressure mixed refrigerant process is 55% higher so the propane-precooled mixed refrigerant process is more efficient in



producing LNG. The propane-precooled mixed refrigerant process is compared between the subcool and flash cycles, resulting in more efficient flash recycle. The effect of LNG feed gas pressure on the process efficiency had been analyzed by Kleemenko (Kleemenko, 1972) based on the feed of pure methane with second law analysis and the optimal liquefaction pressure is around 1000 psia. (Chiu *et al.*, 1980)

### 2.2.1.3 Multistage Cascade Refrigeration Cycle Process

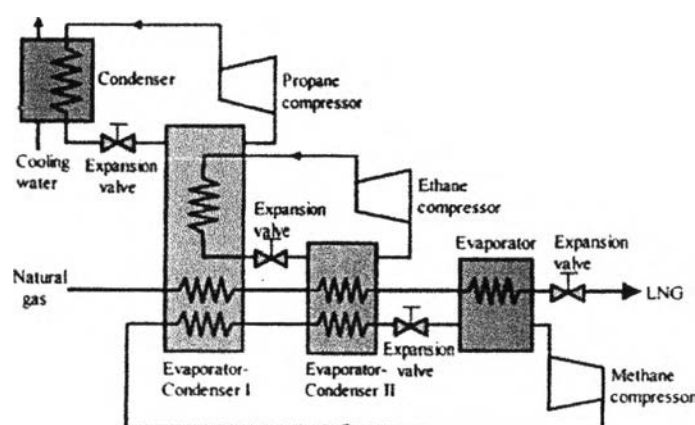


**Figure 2.8** Cascade refrigeration cycle that shows only one stage for each refrigerant cycle (Kanoğlu, 2002).

The operation of cascade refrigeration cycle, as shown in Figure 2.8 consists of three subcycles with different refrigerants. For the first cycle, propane leaves the compressor at high temperature and pressure and enters condenser where cooling water or air is coolant then condensed propane enters the expansion valve where pressure drops to the evaporator pressure. The heat of evaporation of propane is obtained from the condensing ethane, cooling methane, and cooling natural gas. Propane leaves evaporator and enters the compressor to complete the cycle. For the second cycle, the condensed ethane expands in expansion valve and evaporates so methane is condensed and natural gas is further cooled and liquefied. For the third cycle, methane expands and evaporates as natural gas is liquefied and subcooled then methane enters compressor to complete cycle as the pressure of LNG is decreased to storage pressure. The three refrigerant cycles have multistage

compression and expansion with three evaporation temperature for each refrigerant and the mass flow rate in each stage are different. The multiple stages make the temperature different between refrigerants and natural gas are small so it has a smaller exergy losses. The minimum work required per unit mass of natural gas liquefaction increase linearly with decreasing liquefaction temperature. (Kanoğlu, 2002)

#### 2.2.1.4 Single State Mixed Refrigerant Process

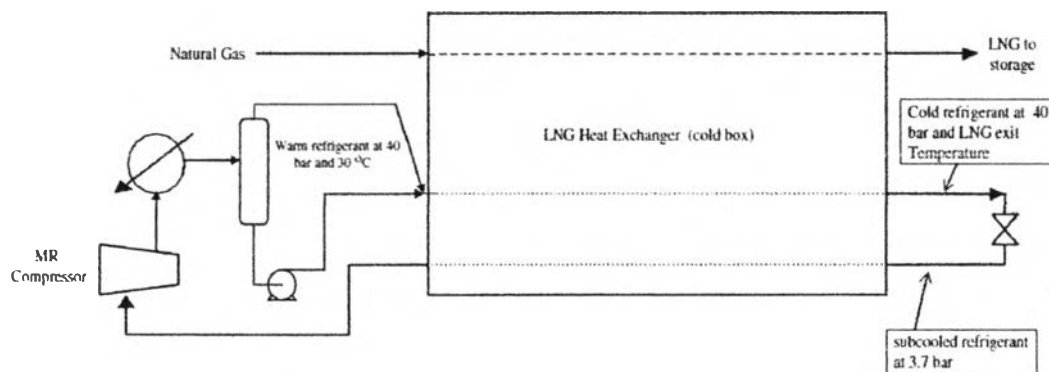


**Figure 2.9** Single-state mixed refrigerant (SMR) (Remelje *et al.*, 2004).

The feed gas enters the LNG exchanger at feed conditions and is cooled by the cold refrigerant stream to reach the LNG storage condition which is less than  $-155\text{ }^{\circ}\text{C}$ , as shown in Figure 2.9. The cold low pressure refrigerant stream is condensed to the high pressure refrigerant stream before the pressure letdown stage, providing the cold side temperature differential of heat exchanger. (Remelje *et al.*, 2004)

#### 2.2.1.5 New LNG Scheme

This new LNG, as shown in Figure 2.10, is more complex than single state mixed refrigerant process that is open-loop scheme where the feed gas is also refrigerant. The low pressure warmed refrigerant gas is recompressed and recycled back to the feed stream that is pre-cooled before splitting into two streams: to be LNG product, and to recycle in refrigerant loop. The external chilling, self-cooling and isentropic expansion is used for cooling and condensation of refrigerant.

The new LNG scheme is more cost effective because using feed gas as refrigerant helped saves as refrigerant cost from using propane (Foglietta, 1999).

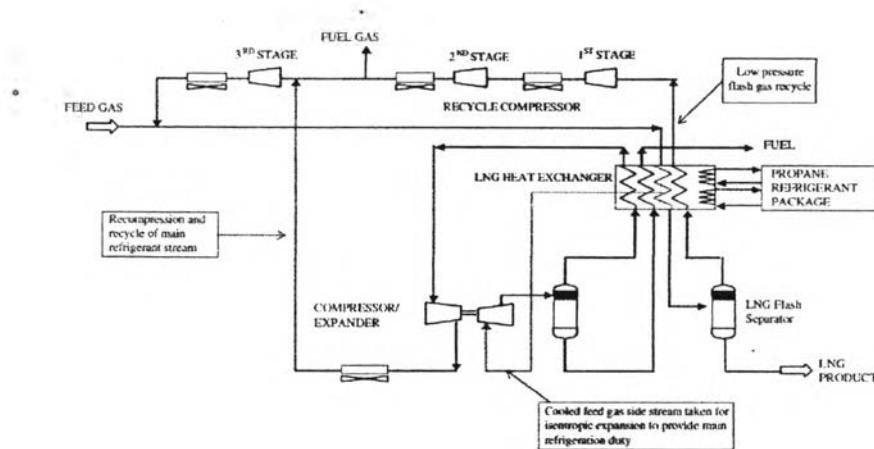


Figure 2.10 New LNG (Foglietta, 1999).

#### 2.2.1.6 GCL Concept

This process, as shown in Figure 2.11, requires exit stream from expander to be liquefied more than 30% by mass. This stream is separated as LNG product and vapor phase is recycled as refrigerant. (Remelje *et al.*, 2004)

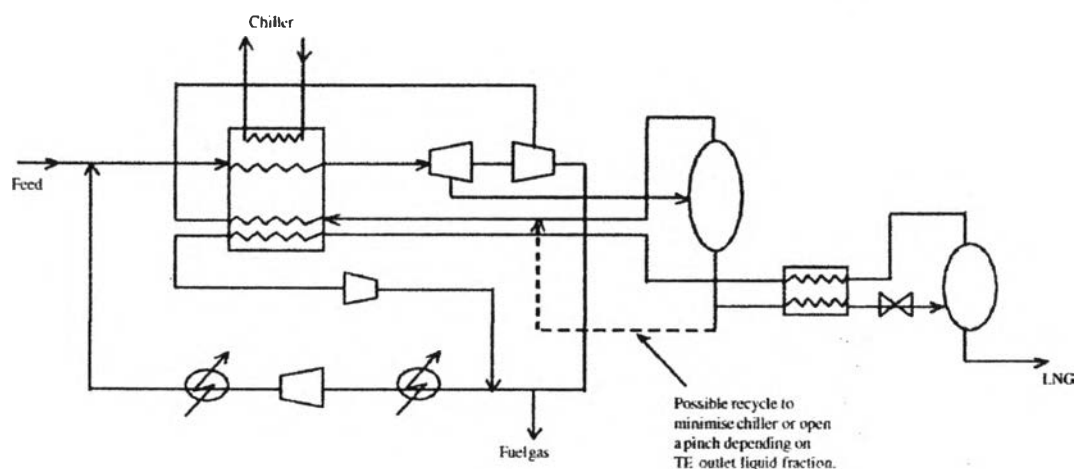


Figure 2.11 The GCL concept (Remelje *et al.*, 2004).

### 2.2.1.7 cLNG

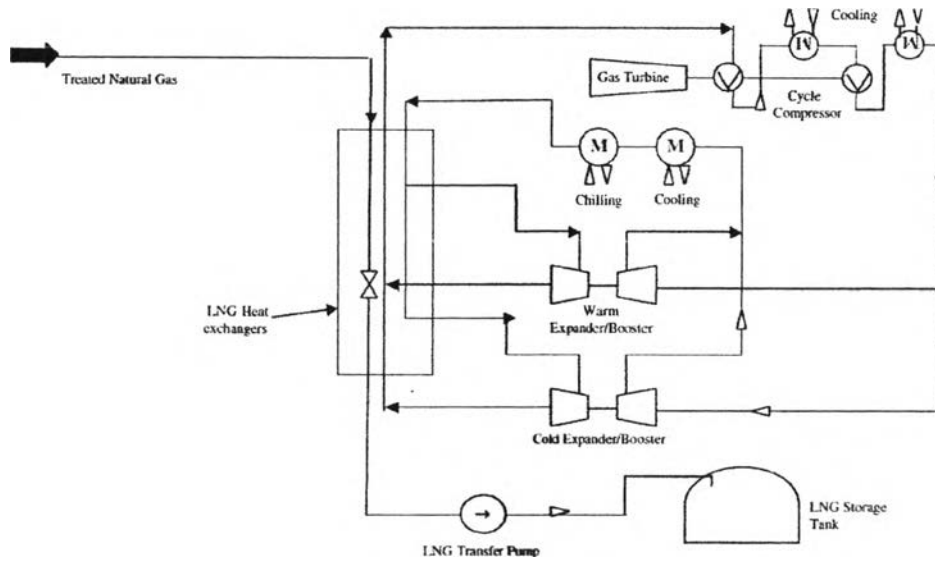


Figure 2.12 The cLNG process (Remeljeje *et al.*, 2004).

This process, as shown in Figure 2.12, uses nitrogen as refrigerant as gaseous phase. The refrigerant is a two-stage system which cool the nitrogen refrigerant to below product temperature using both self-cooling and turbo expander. This technology provides two advantages. One is easier to model because nitrogen is single phase and the other is safer because nitrogen is inert. (Remeljeje *et al.*, 2004)

## 2.3 Fundamental Principles

Consider a refrigerator that provides refrigeration over a constant temperature and operates on reversible thermodynamic processes. Such a refrigerator will henceforth be called a reversible refrigerator as shown in Figure 2.3. Heat is rejected to the surroundings at a temperature  $T_0$  and absorbed at a temperature  $T$ . The first and second laws of thermodynamics can be written for a reversible refrigerator as follows:

First law: 
$$\dot{W}_{r,rev} = \dot{Q} + \dot{Q}_0 \quad (2.15)$$

Second law: 
$$\frac{\dot{Q}}{T} + \frac{\dot{Q}_0}{T_0} = 0 \quad (2.16)$$

Substituting equation (2.16) into equation (2.15) gives the expression for the power required by reversible refrigerator as follows:

$$-\dot{W}_{r,rev} = \dot{Q} \left( \frac{T_0}{T} - 1 \right) \quad (2.17)$$

Where  $T$  and  $T_0$  refer to the refrigeration and ambient temperatures, respectively.  $\dot{Q}$  and  $-\dot{Q}_0$  are the heat absorbed and heat rejected respectively.

The coefficient of performance (COP) of any refrigerator is defined as follows:

$$COP = \frac{\text{heat absorbed at low temperature}}{\text{compressor work input}} = \frac{Q}{-W_c} = \frac{\dot{Q}}{-\dot{W}_c} \quad (2.18)$$

Where  $Q$  and  $-W_c$  refer to the heat absorbed and compressor work input in joules, and  $\dot{Q}$  and  $-\dot{W}_c$  refer to heat transfer rate from the low temperature source and power supplied to the compressor in watts. The coefficient of performance (COP) of an ideal reversible refrigerator providing refrigeration at constant temperature can be expressed in terms of the temperatures for the heat source and heat sink using equation as follows:

$$COP_{r,rev} = \frac{\dot{Q}}{-\dot{W}_{r,rev}} = \frac{T}{T_0 - T} \quad (2.19)$$

### 2.3.1 Pinch Technology

The Pinch technology is a tool to optimize the energy in the industrial processes. A Pinch analysis starts with the heat and material balances for the process. By using Pinch technology, it is possible to identify appropriate changes in the core process conditions that can have an impact on energy savings. The data derived from process consist of hot streams which are sources of heat and cold streams which are sinks of heat. Therefore, the hot and cold composite curves can be drawn and each one will describe the heat demanded and offered in the process.

The composite curves can be plotted on a common temperature-enthalpy diagram as shown in Figure 2.13. The closest approximation between them represents the minimum temperature gradient and it is named the pinch point. The pinch point divides the curves in two different zones: Temperatures above the Pinch

where there is a deficit of thermal load and temperature below the Pinch where there is an excess of thermal load. In the composite curves it is possible to set also the minimum requirements of cooling and heating. The changes in the temperature conditions and mass flow of the process streams have an effect in the behavior of composite curves.

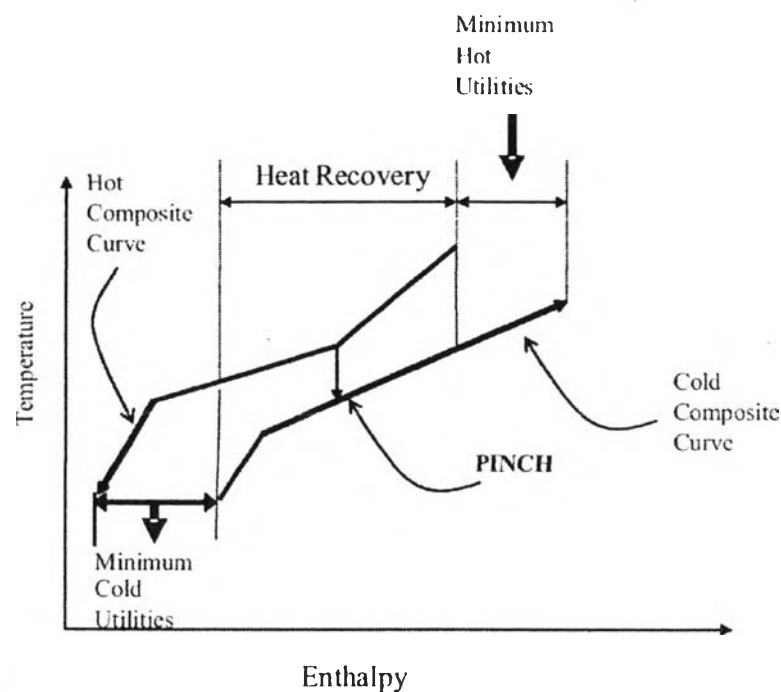


**Figure 2.13** The composite curve of process (Alejandro, 2014).

### 2.3.2 Exergy Analysis

Thermodynamics is founded on its main laws. The first law is the law conservation of energy which the difference between total energy inlet and total energy leaving the system associate with either material stream or energy transfer by work (W) or heat (Q) as below.

$$\frac{dE_{CV}}{dt} = \dot{Q}_0 + \sum_{i=1}^n \dot{Q}_i - w + \sum \dot{m}_i h_{tot,i} - \sum \dot{m}_e h_{tot,e} \quad (2.20)$$

where subscript *i* is inlet, *e* is exit or outlet, *h* is enthalpy and *m* is mass flowrate

The second law is associated with the direction of a process defined as below where *S* is entropy.

$$\Delta \dot{S}_{gen,tot} = \frac{dS_{cv}}{dt} - \sum \dot{m}_i S_i + \sum \dot{m}_e S_e - \frac{\dot{Q}_0}{T_0} - \sum_{i=1}^n \frac{\dot{Q}_i}{T_i} \quad (2.21)$$

Ignore  $\dot{Q}_0$  from equation (2.20) and (2.21) so obtained equation (2.22) as given:

$$\dot{W} = -\frac{d(E-T_0S)_{cv}}{dt} + \sum_{i=1}^n \left(1 - \frac{T_0}{T_i}\right) \dot{Q}_i + \sum \dot{m}_i (h_{tot} - T_0S)_i - \sum \dot{m}_e (h_{tot} - T_0S)_e - T_0 \Delta \dot{S}_{gen,tot} \quad (2.22)$$

For reversible process term  $T_0 \Delta \dot{S}_{gen,tot} = 0$ ;

$$\dot{W}_{rev} = -\frac{d(E-T_0S)_{cv}}{dt} + \sum_{i=1}^n \left(1 - \frac{T_0}{T_i}\right) \dot{Q}_i + \sum \dot{m}_i (h_{tot} - T_0S)_i - \sum \dot{m}_e (h_{tot} - T_0S)_e \quad (2.23)$$

Where useful work defined as  $\dot{W}_U = \dot{W} - P_0 \frac{dV}{dt}$  so that

$$\dot{W}_U = -\frac{d(E+P_0V-T_0S)_{cv}}{dt} + \sum_{i=1}^n \left(1 - \frac{T_0}{T_i}\right) \dot{Q}_i + \sum \dot{m}_i (h_{tot} - T_0S)_i - \sum \dot{m}_e (h_{tot} - T_0S)_e - T_0 \Delta \dot{S}_{gen,tot} \quad (2.24)$$

For reversible process;

$$\dot{W}_{u,rev} = -\frac{d(E+P_0V-T_0S)_{cv}}{dt} + \sum_{i=1}^n \left(1 - \frac{T_0}{T_i}\right) \dot{Q}_i + \sum \dot{m}_i (h_{tot} - T_0S)_i - \sum \dot{m}_e (h_{tot} - T_0S)_e \quad (2.25)$$

$$\text{So that; } \dot{W}_U = \dot{W}_{u,rev} - T_0 \Delta \dot{S}_{gen,tot} \quad (2.26)$$

$$\dot{W}_U = \dot{W}_{u,rev} - I \quad (2.27)$$

where I is work lost or in term exergy is exergy destruction

For the exergy is defined as;

$$\dot{W}_U = -\frac{d(E+P_0V-T_0S)_{cv}}{dt} + \sum_{i=1}^n \left(1 - \frac{T_0}{T_i}\right) \dot{Q}_i + \sum \dot{m}_i (h_{tot} - T_0S)_i - \sum \dot{m}_e (h_{tot} - T_0S)_e - I \quad (2.28)$$

Where defined  $\dot{E}_{Qi} = \left(1 - \frac{T_0}{T_i}\right) \dot{Q}_i$  which is the exergy transfer associated with heat while  $\dot{W}_U$  is exergy transfer accompanying the work interaction equal to electrical or mechanical.

For the exergy balance in open system; steady state  $\frac{d(E+P_0V-T_0S)_{cv}}{dt} = 0$  and

also defined the exergy of process stream per unit mass as:

$$e = (h_{tot} - h_{tot,0}) - T_0(S - S_0) \quad (2.29)$$

and the exergy balance that obtained maximum work from system as shown in Figure 2.14 according to equation (2.30).

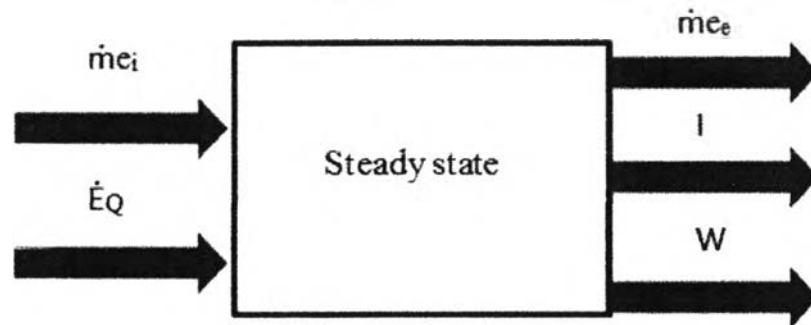


**Figure 2.14** The exergy balance that obtained maximum work from system.

$$0 = \sum_{i=1}^n \dot{E}_{Qi} - \dot{W}_U + \sum \dot{m}_i e_i - \sum \dot{m}_e e_e - I \quad (2.30)$$

The exergy balance that required minimum work as shown in Figure 2.15 according to equation (2.31).

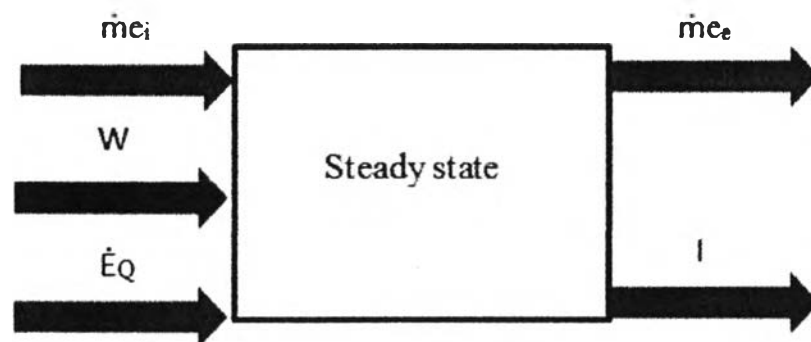


**Figure 2.15** The exergy balance that required minimum work.

$$0 = \sum_{i=1}^n \dot{E}_{Qi} + \dot{W}_U + \sum \dot{m}_i e_i - \sum \dot{m}_e e_e - I \quad (2.31)$$



### 2.3.2.1 Exergy Analysis of Heat Recovery Systems

#### 2.3.2.1.1 Exergy of Process Streams

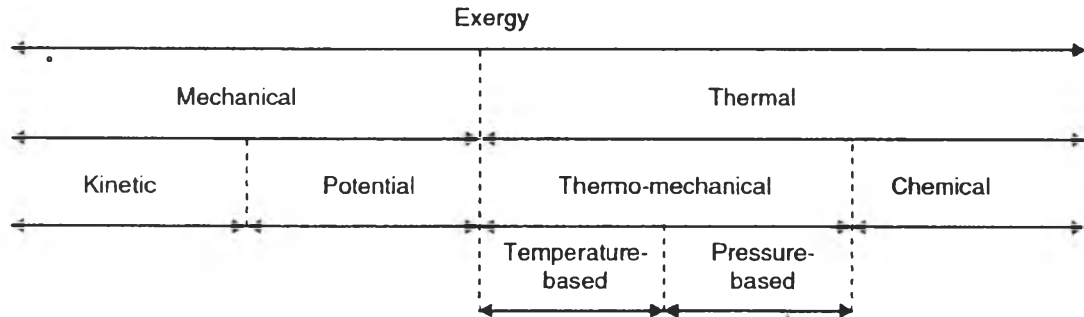


Figure 2.16 Classification of exergy (Aspelund *et al.*, 2007).

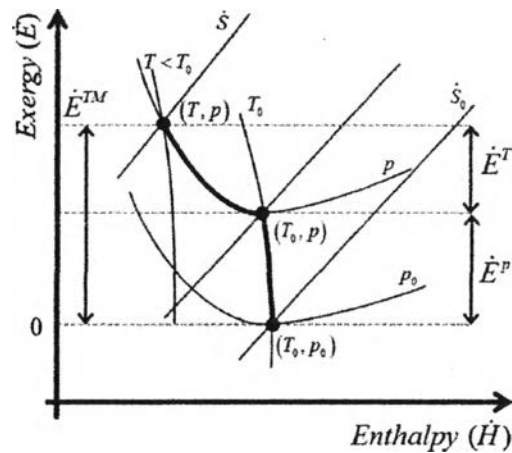


Figure 2.17 Exergy-Enthalpy diagram with decomposition of thermomechanical exergy  $\dot{E}^{TM}$  (Gundersen *et al.*, 2013).

Exergy can be classified into 4 major groups as shown in Figure 2.16: kinetic, potential, thermo-mechanical and chemical due to kinetic and potential energy are forms of mechanical energy can be converted directly into work. Kinetic energy, itself is the work potential or exergy of kinetic and it is independent of temperature and pressure so that kinetic and potential exergy of streams in heat recovery system can be neglect due to small changing. The process

does not involve with reaction, chemical term can neglect also. Thermo- mechanical ( $\dot{E}^{TM}$ ) can be decomposed into pressure based part ( $\dot{E}^P$ ) and temperature based part ( $\dot{E}^T$ ) for the accuracy of exergy analysis due to the process stream is under change of state from  $(T_1, P_1)$  to  $(T_2, P_2)$ . Figure 2.17 shows this exergy decomposition graphically.

The thermo-mechanical exergy is written as:

$$\dot{E}^{TM}(T, P) = \dot{E}^T + \dot{E}^P = \dot{H}(T, P) - \dot{H}(T_0, P_0) - T_0[\dot{S}(T, P) - \dot{S}(T_0, P_0)] \quad (2.32)$$

$$\dot{E}^T(T, P) = \dot{H}(T, P) - \dot{H}(T_0, P) - T_0[\dot{S}(T, P) - \dot{S}(T_0, P)] \quad (2.33)$$

$$\dot{E}^P(T, P) = \dot{H}(T_0, P) - \dot{H}(T_0, P_0) - T_0[\dot{S}(T_0, P) - \dot{S}(T_0, P_0)] \quad (2.34)$$

### 2.3.2.1.2 Exergy of Heat

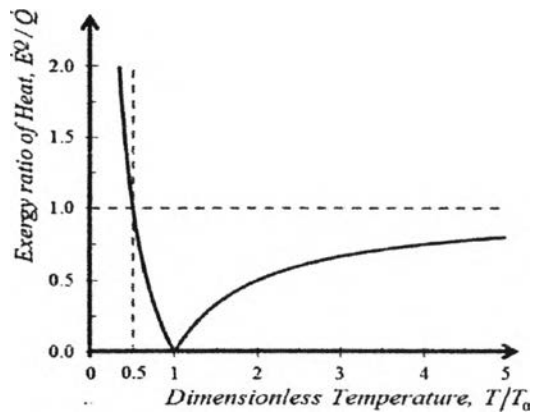


**Figure 2.18** Dimensionless exergy of heat temperature diagram (Gundersen *et al.*, 2013).

The exergy of heat depends on temperature. In Figure 2.18, it is shown that the exergy of heat above  $T_0$  is horizontally asymptotic to  $\dot{Q}$  in equation (2.35); the minimum work produced even by an ideal (reversible) heat engine will always be less than the energy supplied by the heat reservoir ( $\dot{Q}$ ). Below  $T_0$ , the exergy of heat is vertically asymptotic to zero in equation (2.36); the minimum work required to take  $\dot{Q}$  from  $T_0$  to lower temperature can be equal or larger than  $\dot{Q}$  (at  $T = 0$  K, an infinite amount of work is required). Actually, for

temperatures below half of  $T_0$ , the ratio between  $\dot{E}^Q$  and  $\dot{Q}$  is larger than one as shown in Figure 2.18, meaning that heat is more valuable than work.

$$\dot{E}^Q = \dot{Q} \left(1 - \frac{T_0}{T}\right) \text{ for } T \geq T_0 \quad (2.35)$$

$$\dot{E}^Q = \dot{Q} \left(\frac{T_0}{T} - 1\right) \text{ for } T \leq T_0 \quad (2.36)$$

### 2.3.2.2 The Application of Exergy Analysis

The maximum amount of work that can be obtained from a given form of energy using the environmental parameters as reference state is called exergy. The specific flow exergy of a fluid at any cycle is obtained from equation (2.37).

$$e = h - h_0 - T_0(s - s_0) \quad (2.37)$$

where  $T_0$  is the dead state temperature,  $h$  and  $s$  are the enthalpy and entropy of fluid at specified state and  $h_0$  and  $s_0$  are properties at dead state. When multiple the specific flow exergy by mass flow rate gives the exergy rate

$$\dot{E} = \dot{m}e \quad (2.38)$$

The change of exergy shown below represents the minimum amount of work is added or removed to change from state 1 to state 2 when there is increase or decrease in internal energy or enthalpy resulting from the change. (Remelje *et al.*,2004)

$$\Delta e = (h - T_0s)_{state 2} - (h - T_0s)_{state 1} \quad (2.39)$$

There are two types of exergy losses. First, exergy losses include a) diffusive heat losses from process equipment and pipelines (insufficient insulation) b) heat exchange with environment (cooler using air, freshwater or sea water) c) energy content (thermal and/or chemical) in material streams that are not utilized (exhaust gases, purge gases, etc.). Such losses can be referred to as external losses. Second, the destruction of exergy is caused by irreversibilities within the process that referred as internal losses. Irreversibilities are caused by finite driving force and dissipative effects (friction and diffusion) and spontaneous processes (combustion). (Gundersen *et al.*,2012) The exergy destroyed in the system as the difference of incoming and outgoing streams as

$$\dot{i} = \dot{E}_{in} - \dot{E}_{out} \quad (2.40)$$

Refer multistage cascade refrigeration cycle as shown in Figure 2.8, considering evaporators and condensers, they are essentially heat exchangers designed to perform different tasks. In the cycle consists of four evaporators-condensers system. The first, evaporator-condenser I, is the evaporation of propane cycle and the condenser of ethane and methane cycles that express the exergy destruction.

$$\dot{i} = [\sum(\dot{m}_p e_p) + \sum(\dot{m}_e e_e) + \sum(\dot{m}_m e_m) + \dot{m}_n e_n]_{in} - [\sum(\dot{m}_p e_p) + \sum(\dot{m}_e e_e) + \sum(\dot{m}_m e_m) + \dot{m}_n e_n]_{out} \quad (2.41)$$

Where the subscripts in, out, p, e, m and n are inlet, outlet, propane, ethane, methane, and natural gas, respectively. The summation signs are due to there are three stages in each refrigerant cycle with different pressures, evaporation temperatures, and mass flow rates.

For evaporator-condenser II, the exergy destruction is expressed

$$\dot{i} = [\sum(\dot{m}_e e_e) + \sum(\dot{m}_m e_m) + \dot{m}_n e_n]_{in} - [\sum(\dot{m}_e e_e) + \sum(\dot{m}_m e_m) + \dot{m}_n e_n]_{out} \quad (2.42)$$

For the evaporator of methane cycle, the exergy destruction is expressed

$$\dot{i} = [\sum(\dot{m}_m e_m) + \dot{m}_n e_n]_{in} - [\sum(\dot{m}_m e_m) + \dot{m}_n e_n]_{out} \quad (2.43)$$

For the condenser of propane cycle, the exergy destruction is expressed

$$\dot{i} = [\sum(\dot{m}_p e_p) + \dot{m}_n e_n]_{in} - [\sum(\dot{m}_p e_p) + \dot{m}_n e_n]_{out} \quad (2.44)$$

There is one multistage compressor in the cycle for each refrigerant. The total work consumed in the cycle is the sum of work inputs to the compressors. If irreversibilities are totally eliminated, there will be no exergy destruction in a compressor that lead to a minimum work input for the compressor. In reality, there will be irreversibilities due to friction, heat loss, and other dissipative effects. The exergy destruction in propane, ethane, and methane compressor are expressed.

$$\dot{i}_p = \sum(\dot{m}_p e_p)_{in} + \dot{W}_{p,in} - \sum(\dot{m}_p e_p)_{out} \quad (2.45)$$

$$\dot{i}_e = \sum(\dot{m}_e e_e)_{in} + \dot{W}_{e,in} - \sum(\dot{m}_e e_e)_{out} \quad (2.46)$$

$$\dot{i}_m = \sum(\dot{m}_m e_m)_{in} + \dot{W}_{m,in} - \sum(\dot{m}_m e_m)_{out} \quad (2.47)$$

Where  $\dot{W}_{p,in}$ ,  $\dot{W}_{e,in}$ , and  $\dot{W}_{m,in}$  are the actual power inputs to the propane, ethane, and methane compressor, respectively.

For expansion valves, they are used to drop the pressure of LNG to storage pressure. The exergy destruction for propane, ethane, methane, and LNG expansion valves are expressed.

$$\dot{I}_p = \sum(\dot{m}_p e_p)_{in} - \sum(\dot{m}_p e_p)_{out} \quad (2.48)$$

$$\dot{I}_e = \sum(\dot{m}_e e_e)_{in} - \sum(\dot{m}_e e_e)_{out} \quad (2.49)$$

$$\dot{I}_m = \sum(\dot{m}_m e_m)_{in} - \sum(\dot{m}_m e_m)_{out} \quad (2.50)$$

$$\dot{I}_n = \sum(\dot{m}_n e_n)_{in} - \sum(\dot{m}_n e_n)_{out} \quad (2.51)$$

The exergy efficiency of cycle can be defined as

$$\varepsilon = \frac{\dot{W}_{actual} - \dot{I}_{total}}{\dot{W}_{actual}} = \frac{\dot{W}_{min}}{\dot{W}_{actual}} \quad (2.52)$$

$$\dot{W}_{actual} = \dot{W}_{p,in} + \dot{W}_{e,in} + \dot{W}_{m,in} \quad (2.53)$$

Where the exergy difference or the actual work input to cycle that is the sum of the work inputs to compressors minus the total exergy destructions in condensers, evaporators, compressors, and expansion valves.  $\dot{W}_{min}$  is the minimum work input to the cycle.

To evaluate the minimum work can utilize a reversible or Carnot refrigeration. The minimum work input for the liquefaction process of multistage cascade refrigeration cycle as mention above is simply the work input required for operation of Carnot refrigerator for a given heat removal that can be expressed as

$$W_{min} = \int dq \left(1 - \frac{T_0}{T}\right) \quad (2.54)$$

Where  $dq$  is the differential heat transfer and  $T$  is the instantaneous temperature at the boundary where the heat transfer take place. Note that  $T$  is smaller than  $T_0$  so take a negative sign to heat transfer in order to get a positive work input since it is a heat output.

To remove heat from natural gas can be achieved by three Carnot refrigerator as shown in Figure 2.19 (a). The first Carnot refrigerator receives heat from the natural gas and supplies it to the heat sink at  $T_0$  as the natural gas is cooled from  $T_1$  to  $T_2$  and for the other cycles are repeated completely to exist as LNG. The amount of power for supplying each Carnot refrigerator can be determined.

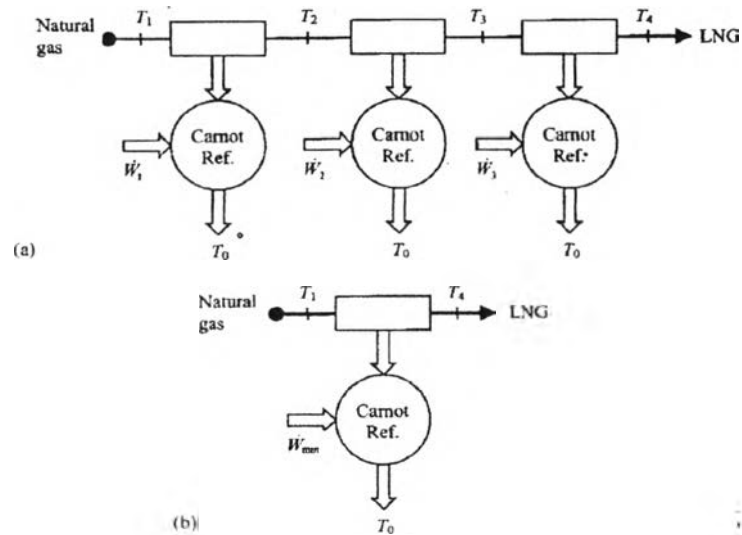


**Figure 2.19** (a) The system used in development of minimum work required for liquefaction of natural gas (b) The system that is equivalent to the system given in (a) (Kanoğlu, 2002).

$$\dot{W}_1 = \dot{m}_n(e_1 - e_2) = \dot{m}_n[h_1 - h_2 - T_0(s_1 - s_2)] \quad (2.55)$$

$$\dot{W}_2 = \dot{m}_n(e_2 - e_3) = \dot{m}_n[h_2 - h_3 - T_0(s_2 - s_3)] \quad (2.56)$$

$$\dot{W}_3 = \dot{m}_n(e_3 - e_4) = \dot{m}_n[h_3 - h_4 - T_0(s_3 - s_4)] \quad (2.57)$$

Where  $\dot{W}_1$ ,  $\dot{W}_2$ , and  $\dot{W}_3$  are the power inputs to the first, second, and third Carnot refrigerators. So the total power input as the minimum power input for the liquefaction process can be determined

$$\dot{W}_{min} = \dot{W}_1 + \dot{W}_2 + \dot{W}_3 = \dot{m}_n(e_1 - e_4) = \dot{m}_n[h_1 - h_4 - T_0(S_1 - S_4)] \quad (2.58)$$

## 2.4 Methods and Tools for Cryogenic Process

In subambient process, pressure is more important design variable because phase change link temperature to pressure through evaporation and condensation and pressure change link temperature to power through expansion.

There are several methods and tools for the cryogenic process.

### 2.4.1 Shaft Work Targeting

The design of a chemical process shows in term of onion diagram as shown in Figure 2.19. The design starts with core process to yield the heat and material balance. The energy target is evaluated by Pinch analysis which indicated by shaded area. Therefore, the utility heat load targets are set directly from a process heat and material balance. However, utility requirements involve power as well as heat. Pinch analysis only involves heat load targets; power component is the limitation especially in low temperature process as shown in Figure 2.21.

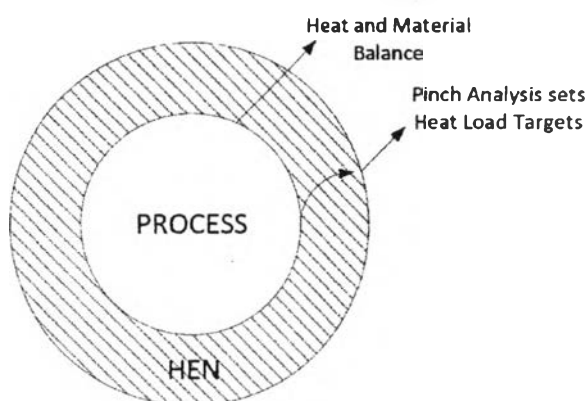


**Figure 2.20** The design of chemical processes (Linnhoff *et al.*,1990).

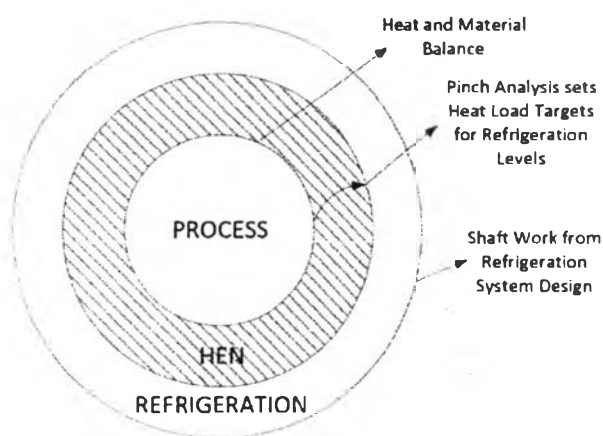


**Figure 2.21** The onion diagram of subambient process (Linnhoff *et al.*,1990).

Linnhoff and Dhole (1990) had introduced the concept of “shaft work targets”, which allows the designer to obtain quantitative changes in the refrigeration shaft work requirement with exergy analysis and bypass the exact design of both HEN and refrigeration system. To show the exergy loss in a heat exchanger network, Carnot factor has been used to form the grand composite curve (EGCCs) as shown in Figure 2.22.

$$\eta_c = 1 - \frac{T_0}{T} \quad (2.59)$$

Where  $\eta_c$  is the Carnot efficiency and  $T_0$  is the environment temperature.

In Figure 2.22, assumed with no change in the process but in the HEN and refrigeration only. Therefore, case A and B have the same EGCCs but different refrigeration profiles. Consider case A in the bar chart.  $\Delta EX_p = X$  and  $(\sigma T_0)_{HEN}$  (shaded area) =  $Y$  so  $\Delta EX_r$  (supplied to HEN) =  $X+Y$ . The loss in the refrigeration system represents in equation where  $\eta_{ex}$  is the exergetic efficiency of refrigeration system and  $W_A$  is the shaft work for case A.

$$W_A = \frac{1}{\eta_{ex}} (X + Y) \quad (2.60)$$

In case B, a new refrigeration level is introduced and corresponding modification in HEN.  $\Delta EX_p = X$  since dealing with the same process.  $(\sigma T_0)_{HEN}$  is reduced by  $Z$  so  $\Delta EX_r = X+Y-Z$ . In equation (2.61) where  $W_B$  is the shaft work for case B.

$$W_B = \frac{1}{\eta_{ex}} (X + Y - Z) \quad (2.61)$$

$\Delta W$  is the reduction in shaft work from case A to case B represents in equation.

$$\Delta W = W_A - W_B = \frac{1}{\eta_{ex}} (Z) \quad (2.62)$$

In other words, the shaded area between curves is proportional to the exergy loss in the HEN and is denoted as  $(\sigma T_0)_{HEN}$ . Thus the amount of ideal work equivalent lost in heat transfer is proportional to the shaded area. When the reduction of shaded area is  $(\sigma T_0)_{HEN}$ , the reduction of the shaft work is

$$\Delta W = \frac{\Delta(\sigma T_0)_{HEN}}{\eta_{ex}} \quad (2.63)$$



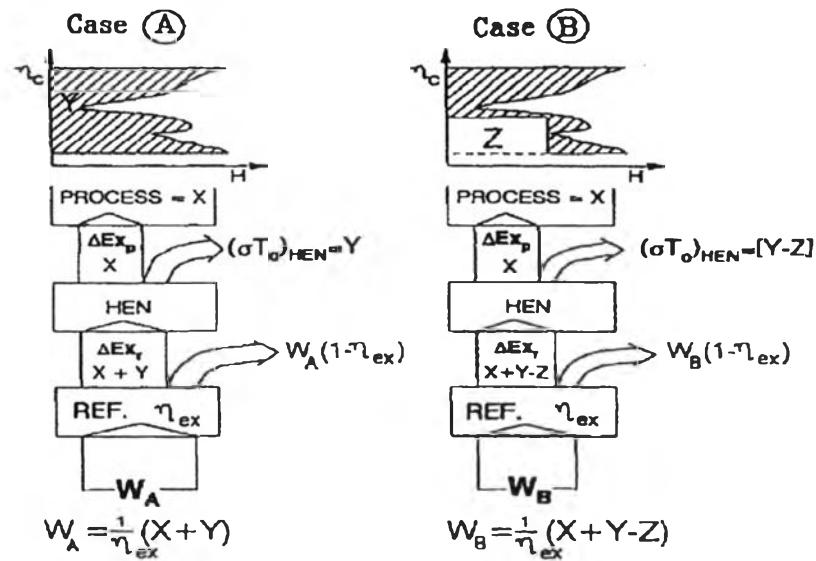


**Figure 2.22** Changes in shaft work are directly related to changes in the shaded area (Linnhoff *et al.*, 1990).

Linnhoff (1994) is introduced an overall design of low temperature processes by utilizing the combination of pinch and exergy. A low temperature process consists of three components; processes, heat exchange system, refrigeration system. Due to all three components are interlinked and interactive, the proposed is resolve these interactions and combine all three components in one design task that based on a combination of pinch analysis and exergy analysis. This process consists of two distillation columns with Carnot factor-enthalpy ( $\eta_c$ -H). The Exergy Grand Composite Curve (EGCCs) as shown in Figure 2.23 represents the overall process exergy balance. The utility system provides exergy, part of which is lost in heat exchange (area between EGCCs and utility levels,  $(\sigma T_0)_{HEN}$ ). The remainder is supplied to the process (area inside EGCCs,  $\Delta Ex_{process}$ ). For subambient, the refrigeration system is the utility system. Linnhoff and Dhole (1992) have shown that changes in the area representing  $(\sigma T_0)_{HEN}$  are proportional to the changes refrigeration shaft work requirement, the proportionality constant being the inverse of the exergy efficiency ( $\eta_{ex}$ ) of refrigeration system. The change in  $(\sigma T_0)_{HEN}$  direct to changes in refrigeration shaft work requirement. The bar chart as shown in Figure 2.24 is represented the concept of low temperature process design. The refrigeration

system provides the overall exergy and the portion is lost in heat transfer  $(\sigma T_0)_{HEN}$  then the remainder is supplied to the process  $(\Delta Ex_{process})$ . Moreover, a part of  $\Delta Ex_{process}$  is lost as process losses then remainder is supplied to the process as minimum theoretical requirement called process core. The reduction in overall area will reduce proportionally in the refrigeration shaft work requirement. The area of  $(\sigma T_0)_{HEN}$  outline is the scope for HEN refrigeration system modifications.

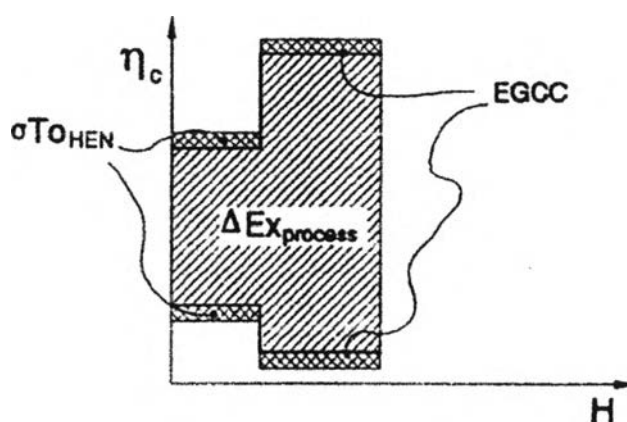


Figure 2.23 The EGCCs representation (Linnhoff *et al.*, 1994).

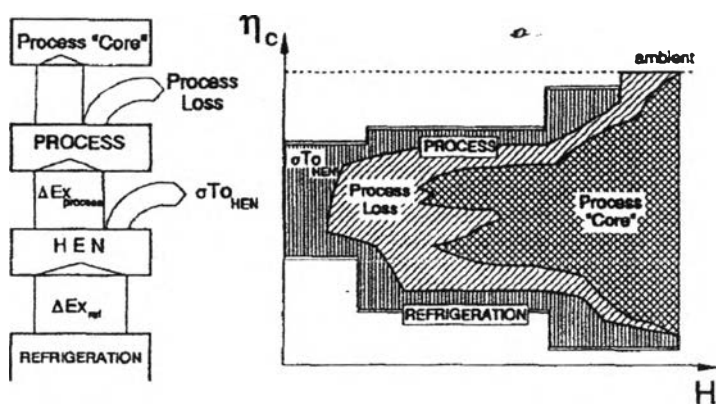


Figure 2.24 Overall exergy balance for a subambient plant (Linnhoff *et al.*, 1994).

#### 2.4.2 Heuristic Rules to Support Subambient Process Design

The heuristic rules are used in pinch analysis based on the fundamental pinch decomposition. A set of 10 heuristic rules address the following issues. First, compression requires power and reduces external heating. Second, expansion produces power and reduces external cooling. Third, phase changes at constant temperature should be avoided when heating or cooling by a stream with non-constant temperature. Fourth, pressure increased by pumping is preferable to compression. (Aspelund *et al.*,2007)

A set of ten heuristics consist of: Heuristic 1, available pressure ( $P_s > P_T$ ) can be utilized through expansion to reduce cold utilities requirements with power generation. Contrary, lack of pressure ( $P_s < P_T$ ) requires power but it reduces hot utility requirement. Heuristic 2, temperature gap ( $\Delta T > T_{min}$ ) between the hot and cold CCs, result in unnecessary irreversibilities. The pressure of stream may be manipulated to decrease irreversibility. Heuristic 3, compression of vapor or dense phase stream require power and will add heat to system. From PA point of view, compression should be done above pinch point. It should be noted that heuristic 3 refers to case where a stream has to be compressed. The actual amount of hot utility saved depend on compressor inlet temperature (outlet should be above pinch) and possible pinch changes (compression will change the shape of CCs). Heuristic 4, expansion of vapor or dense phase stream in an expander will provide cooling to system and generate power. So expansion should be done below pinch. It is noted that expansion at low temperature will provide less cooling and generate less work than at high temperature but colder outlet temperature can be achieved. The expansion process will modify shape of CCs. Heuristic 5, if expansion of a vapor or dense phase stream above pinch is required, a valve should be used to minimize the increase in utility consumption. Heuristic 6, hot gas or dense phase fluid that is compressed above pinch point cooled to near pinch point temperature and then expanded will decrease the need for both cold and hot utilities and additional work is required. Heuristic 7, a fluid with  $P_s < P_T$  should be compressed in liquid phase if possible to save compressor work. Heuristic 8, in a liquid stream with  $P_s = P_T$  a phase transition is necessary for CCs to be manipulated, since the effect of expansion or compression in liquid phase alone is marginal. Heuristic 9, if cold liquid stream to be

vaporized does not create a pinch point, it should be pumped to avoid vaporization at constant temperature; reduce the total cooling duty and increase the pressure based exergy. Heuristic 10, compression of hot gas stream to be condensed will increase the condensation temperature. The latent heat of vaporization will be reduced. So work is used to increase the driving forces and thereby reduce the heat requirements.

#### 2.4.3 The Extended Pinch Analysis and Design Methodology

This method is focused on utilizing pressure exergy in subambient processes. It also uses exergy calculation and provides step by step procedure that utilizes the insight from the graphical representation. (An Extended Pinch Analysis and Design procedure utilizing pressure bases exergy for subambient cooling) (Aspelund *et al.*,2007)

There are seven steps in the overall design procedure. First, using exergy analysis to determine the total exergy in hot and cold stream in order to verify it is possible to create a process without utilities. If it is not the case, the minimum required work can be found. Second, if it is possible, the estimate for irreversibilities given the minimum temperature differences and equipment efficiencies. Third, using pinch analysis to improve composite curves for hot and cold streams to identify the pinch point and the minimum amount of hot and cold utilities. Fourth, selecting an appropriate heuristic to find the best way of manipulating the pressure. Fifth, developing the expanded pinch curves after expansion and compression of process streams. Sixth, calculate the new exergy efficiency and compare the old and new minimum utility values and evaluate the current design with new exergy efficiency. Seventh, the design procedure is based on heuristics so it does not guarantee global optimality. The exergy analysis will indicate there is room for further improvements of the process.

#### 2.4.4 New Graphical Representation of Exergy

Linnhoff and Dhole (1992) have combined PA and EA methods which are represented in graphical method called Exergy Composite Curves (ECCs) and Exergy Grand Composite Curves (EGCCs) based on Carnot factor as shown in Figure 2.25. An alternative graphical exergy targeting for heat recovery systems. The

exergy availability diagram, the Carnot factor is used as y axis and enthalpy as x axis so called exergy composite curves (ECCs) is used as reference for the appropriate placement of heat engine, heat pumps and refrigeration cycles as energy utilities.

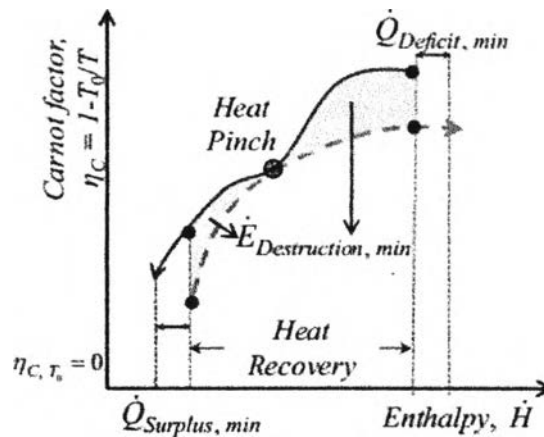


Figure 2.25 ECCs diagram (Gundersen *et al.*, 2012).

In Figure 2.25, the Carnot factor with enthalpy is non-linearly that has drawbacks that are multiple data points must be calculated between supply and target conditions, it is necessary to calculate data for the traditional composite curves for construction of ECCs diagram and exergy analysis of a rather large HRS is a tedious task due to exergy destruction in HRS is equal to area between curves. Second, exergy targets are not explicitly shown in diagrams.

The new exergy is represented by Gundersen *et al.*, 2012, they claim that in process design, the energy availability concept is always implicit in any energy targeting study. For heat recovery system that (i) operates below  $T_0$  and (ii) where streams exhibit pressure changes, the calculation of exergy targets may be high relevant. Exergy of process stream can be transferred in form of temperature based exergy by heating and cooling with another process stream. Moreover,  $\dot{E}^T$  of the streams can also be increased or decreased by correspondingly decreasing or increasing pressure based exergy, trading one for another. For instance, consider a stream that needs to be cooled and expanded below  $T_0$ . The required refrigeration load can be reduced by making use of the cooling provided by expansion. In

addition, shaft work is generated as a byproduct. Thus, there is a need for explicitly obtaining the exergy targets of heat recovery system with operating below  $T_0$ . As a result, the design becomes more efficient processes and easier.

#### 2.4.4.1 Exergetic Temperature

The relationships between the exergy of material streams and their pressure and temperature are nonlinear; therefore, it is not easily visualized. Thus, the specific heat capacity is assumed constant with respect to temperature and pressure for  $\dot{E}^T$  and  $\dot{E}^P$ . In addition ideal gas conditions are assumed constant for  $\dot{E}^P$  in equation (2.34) can be written as equation (2.73). The factors inside the square brackets have the unit temperature (Kelvin, K). These factors are called exergetic temperatures. For  $\dot{E}^T$ , the exergetic temperature ( $T^{E^T}$ ) is only function of temperature and for  $\dot{E}^P$ , the corresponding exergetic temperature ( $T^{E^P}$ ) is only function of pressure. The differential form of Thermo-mechanical exergy is as:

$$dE^{TM} = dE^T + dE^P \quad (2.64)$$

$$dE^{TM} = \left( \frac{\partial E^{TM}}{\partial T} \right)_P \cdot dT + \left( \frac{\partial E^{TM}}{\partial P} \right)_T \cdot dP \quad (2.65)$$

$$dE^T = \left( \frac{\partial E^{TM}}{\partial T} \right)_P \cdot dT = \left[ \left( \frac{\partial h}{\partial T} \right)_P + T_0 \left( \frac{\partial s}{\partial T} \right)_P \right] \cdot dT \quad (2.66)$$

$$dE^P = \left( \frac{\partial E^{TM}}{\partial P} \right)_T \cdot dP = \left[ \left( \frac{\partial h}{\partial P} \right)_T + T_0 \left( \frac{\partial s}{\partial P} \right)_T \right] \cdot dP \quad (2.67)$$

Where,

$$\left( \frac{\partial h}{\partial T} \right)_P = C_p \quad (2.68)$$

$$\left( \frac{\partial s}{\partial T} \right)_P = \frac{C_p}{T} \quad (2.69)$$

$$\left( \frac{\partial h}{\partial P} \right)_T = v - T \left( \frac{\partial v}{\partial T} \right)_P \quad (2.70)$$

$$\left( \frac{\partial s}{\partial P} \right)_T = - \left( \frac{\partial v}{\partial T} \right)_P \quad (2.71)$$

Thus,

$$E^T = \int_{T_0}^T C_p \cdot \left( 1 - \frac{T_0}{T} \right) \cdot dT \quad (2.72)$$

$$E^P = \int_{P_0}^P \left[ v - (T - T_0) \cdot \left( \frac{\partial v}{\partial T} \right)_P \right] \cdot dP \quad (2.73)$$

Assuming specific heat capacity and ideal gas are constant in equations (2.33, 2.34) become equations (2.74, 2.75);

$$\dot{E}^T = \dot{m}C_p \left[ T_0 \left( \frac{T_0}{T} - \ln \frac{T_0}{T} - 1 \right) \right] = \dot{m}C_p T^{E^T} \quad (2.74)$$

$$\dot{E}^P = \dot{m}C_p \left[ T_0 \ln \left( \frac{P}{P_0} \right)^{\frac{\kappa-1}{\kappa}} \right] = \dot{m}C_p T^{E^P} \quad (2.75)$$

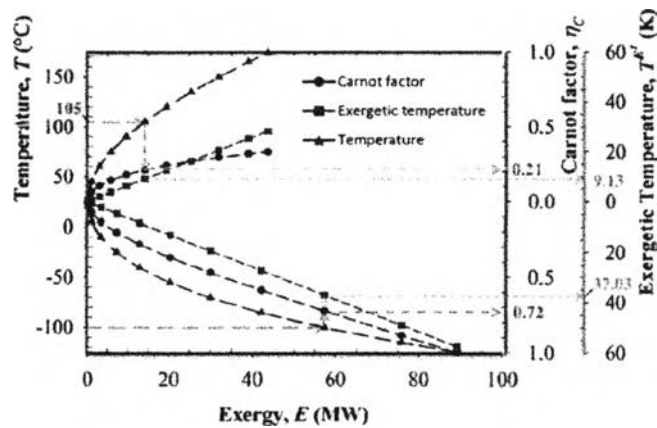


**Figure 2.26** Comparison between exergetic temperature, regular temperature and Carnot factor (Gundersen *et al.*, 2013).

Figure 2.26 shows a comparison between the behavior of the exergetic temperature, the regular temperature scale, and the Carnot factor. Some important features that can observe from Figure are (i) that the exergetic temperature is always positive, (ii) the minimum value is zero at  $T_0$  and (iii) its increase is in linear relation with exergy.

When plotting the exergetic temperatures versus exergy, it is possible to read directly from this diagram the corresponding exergy targets as shown in Figure 2.27.

Some characteristics of diagrams as shown in Figure 2.27, first, exergy sources and sinks are plotted in a composite manner using  $T^{E^T}$  instead of regular supply and target temperature of streams. Second, the coldest temperature ties with the largest exergetic temperature for streams below  $T_0$ . Third, the exergy deficit and surplus figures are calculated ahead of design from the exergy cascade.

Fourth, the heat and exergy pinch points are placed in corresponding enthalpy and exergy intervals. Thus, if the pinch rules are followed, then exergy is not imported below pinch nor exported above pinch, and exergy is not transfer across pinch. Fifth, exergy destruction is shown by transforming the boundary temperatures of the overlapping region obtained in the traditional CCs into exergetic temperatures. The calculations of exergy targets are expressed.

$$\text{Above exergy pinch: } \dot{E}_{\text{Requirement}, \text{min}} = \dot{E}_{\text{Deficit}, \text{min}} + \dot{E}_{\text{Destruction}, \text{min}} \quad (2.76)$$

$$\text{Below exergy pinch: } \dot{E}_{\text{Rejection}, \text{min}} = \dot{E}_{\text{Surplus}, \text{min}} - \dot{E}_{\text{Destruction}, \text{min}} \quad (2.77)$$

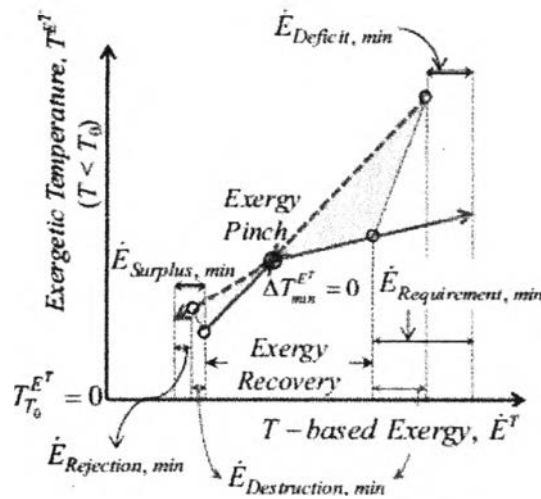


Figure 2.27  $T^{E^T} - \dot{E}^T$  diagram below  $T_0$  (Gundersen *et al.*, 2012).

## 2.5 Mathematical Programming

Nowadays the design and optimization procedure have the trend to identify the configurations where the less energy consumption and economic saving can be achieved. The optimization of the Heat Exchanger Networks required for integration of the refrigeration system with process streams. Yee and Grossmann (1990) proposed MINLP model based on the superstructure representation. The binary variable as 0-1 can be handled with constraint on stream splitting that solved with solvers for isothermal mixing assumption.



The series paper of simultaneous optimization models for heat integration by Yee and Grossmann, (1990) is divided into three parts.

In first part of Yee *et al.* (1990), a stage-wise superstructure is first presented and developed for various heat integration problems. The proposed representation does not rely on any heuristics. The objective function for simultaneous optimization of energy and area targets involves utilities and area cost. They demonstrated that the simultaneous model can trade-offs between utilities and area cost. If the utility requirement for network is fixed, the simultaneous model modified to only minimize total area requirement is called area targeting model. In the last section, the proposed model for area targeting is applied for the modeling of multistream heat exchangers.

In second part of Yee and Grossmann, (1990), a mixed integer nonlinear programming (MINLP) model is derived from the superstructure representation proposed in part I. MINLP model can generate networks where utility cost, exchanger area and fixed charge for the number of units are optimized simultaneously. Because of the assumption of isothermal mixing, the constraints of MINLP model, optimizing simultaneously for the heat recovery approach temperature (HRAT), the exchanger minimum approach temperature (EMAT), number of units, number of splits and heat transfer area, are set of linear constraints. In addition, the model is possible to match pairs of hot streams or pairs of cold streams as well as variable inlet and outlet temperatures. Several examples show that some heuristic rules do not achieve when optimization is performed simultaneously

In third part of Yee *et al.* (1990), to simultaneously optimize or synthesize of the heat exchanger network and process, the stage-wise representation in part I is embedded into the given process superstructure and, then, optimize the combined model where flow and temperature of potential hot and cold streams as variables and it does not require specification of the heat recovery approach temperature (HRAT), the exchanger minimum approach temperature (EMAT). To design the model, either nonlinear programming (NLP) or mixed integer nonlinear programming (MINLP) is used. For mixed integer nonlinear programming (MINLP), the use of binaries provides an accuracy of HEN capital cost since fixed charges for requiring units can be charged explicitly and can be impose constraints on the network structure.

However, The computational time of mixed integer nonlinear programming is required larger than that of nonlinear programming formulation.